Utility-Optimal Resource Management and Allocation Algorithm for Energy Harvesting Cognitive Radio Sensor Networks

Deyu Zhang, *Student Member, IEEE*, Zhigang Chen, *Member, IEEE*, Mohamad Khattar Awad, *Member, IEEE*, Ning Zhang, *Member, IEEE*, Haibo Zhou, *Member, IEEE*, and Xuemin (Sherman) Shen, *Fellow, IEEE*

***Abstract*— In this paper, we study resource management and allocation for energy harvesting cognitive radio sensor networks (EHCRSNs). In these networks, energy harvesting supplies the network with a continual source of energy to facilitate the self-sustainability of the power-limited sensors. Furthermore, cognitive radio enables access to the underutilized licensed spectrum to mitigate the spectrum-scarcity problem in the unlicensed band. We develop an aggregate network utility optimization framework for the design of an online energy management, spectrum management, and resource allocation algorithm based on Lyapunov optimization. The framework captures three stochastic processes: energy harvesting dynamics, inaccuracy of channel occupancy information, and channel fading. However, *a priori* knowledge of any of these processes statistics is not required. Based on the framework, we propose an online algorithm to achieve two major goals: first, balancing sensors' energy consumption and energy harvesting while stabilizing their data and energy queues; second, optimizing the utilization of the licensed spectrum while maintaining a tolerable collision rate between the licensed subscriber and unlicensed sensors. The performance analysis shows that the proposed algorithm achieves a close-to-optimal aggregate network utility while guaranteeing bounded data and energy queue occupancy. The extensive simulations are conducted to verify the effectiveness of the proposed algorithm and the impact of various network parameters on its performance.**

***Index Terms*— Wireless sensor network, cognitive radio, energy harvesting, energy management, channel allocation, Lyapunov optimization.**

I. Introduction

ENERGY Harvesting Sensor Networks (EHSNs) are promising for long-term data collection over a wide range of applications [1], and become a fundamental enabling technology for the coming era of Big Data [2] and the Internet of Things (IoTs) [3]. By exploiting the EH technology, sensors can harvest energy from the renewable energy sources in the area of interest, such as solar, illumination and vibration [4]. Therefore, it facilitates the self-sustainability of the power-constrained sensors and effectively extends the network lifetime.

EHSNs typically operate on the unlicensed Industrial, Scientific, and Medical (ISM) band for data transmission. However, the ISM band has become increasingly crowded due to the massive growth of wireless devices operating in this band. This massive growth has introduced the spectrum-scarcity problem which significantly degrades the performance of EHSNs. In addition, a large portion of the licensed spectrum remains underutilized, e.g., the spatial and temporal variations in the licensed spectrum utilization range from 15% to 85%, according to a report by Federal Communications Commission [5]. The integration of Cognitive Radio (CR) technology into EHSNs mitigates these licensed spectrum-underutilization and unlicensed spectrum-scarcity problems. It facilitates the transmission of sensed data over the underutilized licensed channels without disrupting the primary network operation. Such networks are referred to as Energy Harvesting Cognitive Radio Sensor Networks (EHCRSNs) in which sensors are secondary users (SUs) and primary network subscribers are primary users (PUs) [6]. The typical applications of EHCRSNs include the data collection indoors, where the sensors overlap with WiFi networks [7], the body sensor networks in pervasive health monitoring, and real-time monitoring in smart city [8]–[10].

Although EHCRSNs are spectrum and energy-efficient, they face several new challenges compared with the traditional sensor networks [11]. First, the energy harvesting process is stochastic and dynamic, which makes balancing energy consumption and energy replenishment challenging. Depleting a sensor's battery at a rate slower or faster than the replenishment rate leads to either energy underutilization or sensor failure, respectively [12]. Second, the spectrum utilization by sensors in EHCRSNs has to adapt to the dynamic activity of PUs over the licensed spectrum [13]. For example, the spectrum occupation of cellular users is in the range of seconds or minutes [14]. When sensors transmit over the channels licensed to cellular users, the sensors may have to frequently disrupt their transmission and vacate the channels to avoid collisions with cellular

Manuscript received January 31, 2016; revised May 15, 2016; accepted August 4, 2016. Date of publication September 20, 2016; date of current version December 29, 2016. This work was supported in part by the Fundamental Research Funds for the Central Universities of the Central South University under Grant 2013zzts043, in part by the Kuwait Foundation for the Advancement of Sciences under Project P314-35EO-01, in part by the National Natural Science Foundation of China under Grant 61379057 and Grant 61272149, and in part by NSERC, Canada. *(Corresponding author: Zhigang Chen.)*

D. Zhang is with the School of Information Science and Engineering, Central South University, Changsha 410083, China (e-mail: zdy876@mail.csu.edu.cn).

Z. Chen is with the School of Software, Central South University, Changsha 410083, China (e-mail: czg@mail.csu.edu.cn).

M. K. Awad is with the Computer Engineering Department, Kuwait University, Kuwait City 13060, Kuwait (e-mail: mohamad@ieee.org).

N. Zhang, H. Zhou, and X. Shen are with the Department of Electrical and Computer Engineering, University of Waterloo, Waterloo, ON N2L 3G1, Canada (e-mail: n35zhang@bbcr.uwaterloo.ca; h53zhou@bbcr.uwaterloo.ca; xshen@bbcr.uwaterloo.ca).

Digital Object Identifier 10.1109/JSAC.2016.2611960

users. Under these highly stochastic and dynamic conditions, managing and allocating resource for EHCRSNs becomes challenging.

To address the above challenges, we develop an aggregate utility optimization framework to facilitate the design of an online algorithm that couples energy management with spectrum access management as well as sensing and transmission rate control for a single-hop EHCRSN. The considered EHCRSN consists of a sink and a number of sensors equipped with EH modules and CR transceivers. The sensors harvest energy to sense data and transmit it to the sink over the unoccupied licensed spectrum. The developed framework is Lyapunov optimization-based, and captures the dynamic and stochastic system of EHCRSN resources. Based on the framework, an online algorithm is designed to achieve a close-to-optimal time-average aggregate network utility, which captures the data sensing efficiency of the network [15], while ensuring protection of PUs and a deterministic bound on the battery capacity of sensors. Summarily, the main contributions of this work are as follows:

1) We propose a stochastic formulation of the network utility optimization problem for the EHCRSN subject to the stability of sensors' data queues and PUs' protection. The proposed formulation accounts for the multiple dynamic and stochastic processes, including the energy consumption of data sensing and transmission, energy harvesting, PU activity on each channel and collisions with sensors, and channel fading.
2) We develop a framework to decompose the problem into three deterministic subproblems: battery management, sampling (i.e., sensing) rate control, and resource (i.e., channel and data rate) allocation on the basis of Lyapunov optimization. Under the developed framework, we propose an online and low-complexity algorithm which makes decisions at the beginning of each time slot and does not require any priori knowledge of the stochastic processes. Furthermore, we apply an unbalanced matching method to assign channels to sensors while considering the limited number of CR transceivers mounted on the sink.
3) We analyze the performance of the proposed algorithm in terms of PU protection and the stability of the sensors data queues. Furthermore, we compute the required battery capacity to support the operation of the proposed algorithm, which depends on the energy consumption of data sensing and transmission. The finding theoretically provides the required capacity of sensors' data buffer and battery for a desired network utility.

The remainder of this paper is organized as follows. Related works are reviewed in Section II. The network model and problem formulation are presented in Section III. The proposed framework is presented in Section IV. Section V analyzes the stability and optimality of the proposed solution. Simulation results are provided to evaluate the performance of the proposed algorithm in Section VI. Section VII concludes this paper and outlines future work.

II. Related Works

Utility-optimal energy management policy design for EHWSNs has been widely addressed in the literature [16]–[20]. Liu *et al.* [18] design two algorithms to optimize the network utility by exploiting convexity of the network flow problem. The first algorithm computes the data sampling rate and routing based on dual decomposition. To deal with the fluctuations in the EH process, the other algorithm maintains the battery at a target level. Zhang *et al.* [19] propose a distributed algorithm to schedule data sensing and perform routing for EHWSNs with limited battery capacity. Furthermore, the proposed algorithm mitigates the estimation error of the EH process by adaptively scheduling the data sensing and routing in each time slot. Zhang *et al.* [20] present two algorithms for balanced energy allocation of sensors, and optimal data sensing and data transmission. Liu *et al.* [18] and Zhang *et al.* [19], [20] assume a priori perfect knowledge of the harvesting process statistics. This may not be practical due to the stochastic nature of EH processes. Huang et al. design an online scheduling algorithm which jointly considers the data routing, admission control and energy management. The algorithm does not require priori knowledge of the EH process and achieves close-to-optimal utility for EHWSNs [17]. Based on the algorithm in [17], Xu *et al.* [16] investigate the utility-optimal data sensing and transmission in EHWSNs with heterogeneous energy sources, i.e., power grids and harvested energy [16]. Xu *et al.* [16] also study the trade-off between achieved network utility and cost on energy from power grid.

Other works exploit the spectrum utilization and performance improvement that CR technologies bring to WSNs and focus on channel allocation for CRSNs [21]–[24]. Ozger *et al.* [22] propose an event-driven clustering protocol for event-to-sink communication coordination in CRSNs. The proposed protocol considers the availability of licensed spectrum in forming cluster, and minimizes the energy consumption for event detection. Li *et al.* [23] investigate the cooperative spectrum sensing schedule for a CRSN, in which sensors decide whether to join spectrum sensing for energy conservation. An evolutionary game is formulated to facilitate the decision of sensors according to their utility history. Ozger *et al.* [22] and Li *et al.* [23], however, do not account for possible collisions between the PUs and SUs; they assume perfect knowledge of the spectrum occupancy. As a result, if spectrum sensing false alarms and detection errors are considered, these approaches cannot be adopted. Unlike in [22] and [23], Urgaonkar and Neely [21] and Qin *et al.* [24] consider the imperfection of channel availability information and design channel allocation algorithms that guarantee the protection of PUs' transmissions against collision. Urgaonkar and Neely [21] develop an opportunistic channel accessing policy for cognitive radio networks to maximize the network throughput by taking the maximum collision constraint in to account. Qin *et al.* [24] optimize the delay and throughput of multi-hop secondary networks in which the secondary users are mounted with multiple CR transceivers.

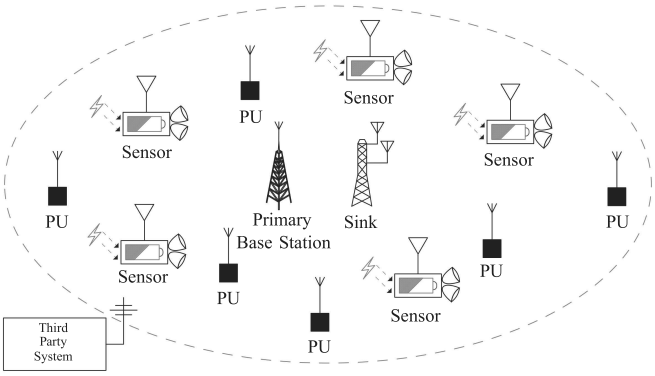

Fig. 1. Illustration of EHCRSN that shows the coexistence of the primary users and the sensor network.

The above-mentioned works either assume availability of spectrum and neglect the spectrum-scarcity problem [16]–[20], or do not consider energy management [21]–[24]. Thus, they cannot fulfill the requirements of EHCRSNs. To fill this research gap, this paper proposes a framework to capture the dynamics of EH process and channel condition, and channel sensing inaccuracy. Based on the framework, a low-complexity algorithm is presented to jointly manage sensors' energy and allocate the channels for network utility optimization.

III. System Model and Problem Formulation

We consider a single-hop EHCRSN of N sensors forming the set $\mathcal{N} = \{1, 2, \cdots, N\}$ and operating over the time slots $t \in \mathcal{T} = \{0, 1, 2, \cdots\}$. As shown in Fig. 1, the EHCRSN coexists with PUs that have the privilege to access licensed channels. The sensor collects data from an area of interest and saves it in its data queue, then transmits it to the sink over licensed channels. There are L transceivers mounted on the sink such that the sink can support L concurrent data transmission over L different frequency bands in each time slot. The availability information of the licensed spectrum is acquired from a third-party system (TPS). The TPS detects the PU activities by various existing spectrum-sensing technologies, such as energy detection [25].

Throughout this paper, we use the following notations. For a random variable X, the expected value is denoted by $\mathbb{E}[X]$, and its conditional expectation on event A is denoted by $\mathbb{E}[X|A]$. The function $[x]^+$ denotes non-negative values, i.e., $\max(x, 0)$.

A. Sampling Rate and Utility

In time slot t, sensor n collects data at a sampling rate $r_n(t)$, which falls in the range:

$$0 \leq r_n(t) \leq r_{max}, \quad \forall n \in \mathcal{N}, \tag{1}$$

where r_{max} is the maximum sampling rate. The sampling rate is associated with a utility function $U(r_n(t))$, which is increasing, continuously differentiable and strictly concave in $r_n(t)$ with a bounded first derivative $U'(r_n(t))$ and $U(0) = 0$ [26]. The concavity of the utility function is based on the observation that the marginal utility of the collected data decreases as the amount of collected data increases in sensor networks [19]. The upper bound of the first-order derivative of $U(r_n(t))$ is denoted by ζ_{max} and equals $U'(0)$.

B. Channel Detection and Allocation Model

The licensed spectrum is divided into K orthogonal channels of equal bandwidth. The set of orthogonal channels is denoted by $\mathcal{K} = \{1, 2, \cdots, K\}$ with cardinality $K = |\mathcal{K}|$. Let $\boldsymbol{S}(t) = (S_1(t), \cdots, S_K(t))$ denote the channel availability indicator with the interpretation that $S_k(t) = 1$ if channel k is available, and $S_k(t) = 0$ otherwise. We assume that the PU activity on channel k evolves following an independent and identical distribution (i.i.d.) across the time slots and is uncorrelated with sensors' activities [21]. The channel unavailability rate which corresponds to the PU activity rate on channel k is given by $\beta_k = \lim_{T\to\infty} \frac{1}{T} \sum_{t=0}^{T-1} (1 - S_k(t)) \leq 1$.

The EHCRSN acquires the availability of channels at the beginning of each time slot from the TPS. Owing to detection errors of spectrum-sensing such as false-alarms and misdetection [27], the channel availability information is assumed to be imperfect. Thus, the TPS provides channel access probability vector $\boldsymbol{Pr}(t) = (Pr_1(t), \cdots, Pr_k(t), \cdots Pr_K(t))$, where $Pr_k(t)$ denotes the probability that channel k is idle and hence accessible in time slot t [21]. Two factors impact the channel access probability: the actual PU activity on channel k, i.e., $S_k(t)$, and the accuracy of the spectrum-sensing techniques [25]. The performance of spectrum sensing techniques highly depends on the receiver signal-to-noise ratio (SNR) and the detection parameters (e.g., detection threshold) [27]. These conditions in the t^{th} time slot are collectively denoted by $\Theta(t)$. The channel access probability $Pr_k(t)$ is the conditional probability of the channel being available in time slot t, i.e., $Pr_k(t) = Pr[S_k(t) = 1|\Theta(t)]$ [21]. Because $S_k(t) = 1$ indicates that the availability of channel k, with $S_k(t) = 0$ otherwise, the closer the value of $\boldsymbol{Pr}(t)$ is to that of $\boldsymbol{S}(t)$, the more accurate the channel availability information is. An EHCRSN with accurate $\boldsymbol{Pr}(t)$ is more efficient in utilizing the licensed channels by avoiding collisions.

At the beginning of each time slot, the sink allocates licensed channels to sensors based on the channel access probability. Let $\mathbf{J}(t)$ denote the channel allocation matrix of elements $J_{n,k}(t), \forall n \in \mathcal{N}, k \in \mathcal{K}$; $J_{n,k}(t) = 1$ if channel k is allocated to sensor n, and otherwise is 0. To avoid interference among sensors, each channel can be allocated to one sensor at most,

$$\sum_{n\in\mathcal{N}} J_{n,k}(t) \leq 1, \quad \forall k \in \mathcal{K}. \tag{2}$$

Furthermore, each sensor can use at most one channel in each time slot, so we have

$$\sum_{k\in\mathcal{K}} J_{n,k}(t) \leq 1, \quad \forall n \in \mathcal{N}. \tag{3}$$

Because there are L transceivers mounted on the sink, the sink can support at most L concurrent data transmissions over licensed channels in each time slot. This can be written as,

$$\sum_{n\in\mathcal{N}} \sum_{k\in\mathcal{K}} J_{n,k}(t) \leq L. \tag{4}$$

C. Collision Control Model

Due to the inaccuracy of channel availability and PU activities, PUs and sensors may collide over the channels. The EHCRSN may access the channel that is occupied by PUs, and thus both data transmissions from PUs and sensors fail due to interference. We assume that the PU on channel k can tolerate a time-average collision rate denoted by ρ_k [21]. For example, $\rho_k = 1\%$ implies that the PU on channel k can tolerant at most 1% of data loss. Recalling that the PU on channel k is active with rate β_k, the target tolerable collision rate evaluates to $\beta_k \rho_k$. Define a collision indicator $C_k(t) \in \{0, 1\}$. The collision indicator takes a value of 1 if collision occurs and is 0 otherwise. A collision occurs when an unavailable channel is allocated to one of the sensors, such that $C_k(t) = (1 - S_k(t)) \sum_{n \in \mathcal{N}} J_{n,k}(t)$. The time-averaged rate of collision between PUs and sensors on the k^{th} channel can be defined as

$$\bar{C}_k = \lim_{T \to \infty} \frac{1}{t} \sum_{t=0}^{T-1} C_k(t), \quad \forall k \in \mathcal{K}.$$

$\bar{C}_k$ should be less than the target tolerable collision rate $\beta_k \rho_k$, i.e.,

$$\bar{C}_k \leq \beta_k \rho_k, \quad \forall k \in \mathcal{K}. \tag{5}$$

To keep track of collisions between sensors and PUs, we define the virtual collision queue $Z_k(t)$ for each channel and a vector of virtual collision queues for all licensed channels, $\boldsymbol{Z}(t) = (Z_1(t), \cdots Z_K(t))$.

The collision queue occupancy varies following a single-server system with the collision variable $C_k(t)$ as an input process and $\rho_k 1_k(t)$ as a service process. $1_k(t)$ here is the complement of the channel availability indicator $1_k(t) = 1 - S_k(t)$. The collision queue occupancy $Z_k(t)$ evolves according to [21]:

$$Z_k(t+1) = [Z_k(t) - \rho_k 1_k(t), 0]^+ + C_k(t), \quad \forall k \in \mathcal{K}, \tag{6}$$

The collision queue is stable only if the time-average input rate $\lim_{t \to \infty} \frac{1}{t} \sum_{\tau=0}^{t-1} C_k(\tau) = \rho_k \beta_k$ is less than the time-average service rate $\lim_{t \to \infty} \rho_k \frac{1}{t} \sum_{\tau=0}^{t-1} (1 - S_k(\tau)) = \bar{C}_k$, i.e.,

$$\lim_{t \to \infty} \frac{1}{t} \sum_{\tau=0}^{t-1} C_k(\tau) \leq \lim_{t \to \infty} \rho_k \frac{1}{t} \sum_{\tau=0}^{t-1} (1 - S_k(\tau)),$$

which is equivalent to the constraint (5). Therefore, stabilizing the collision queue for each channel maintains the required PU protection.

D. Energy Consumption Model

In each time slot, the n^{th} sensor senses data with sampling rate $r_n(t)$ from the area of interest and saves it in the data queue. The energy consumption[1] of data sensing is assumed to be a linear function of the sampling rate $r_n(t)$ [16] and denoted by $P_S r_n(t)$. If channel k is allocated to the n^{th} sensor, it transmits data to the sink with power P_T, $\forall n \in \mathcal{N}$. Thus, the total energy consumption P_n^{total} of the n^{th} sensor in the t^{th} time slot is

$$P_n^{total}(t) = P_S r_n(t) + \sum_{k \in \mathcal{K}} J_{n,k}(t) P_T, \quad \forall n \in \mathcal{N}.$$

Because the sampling rate $r_n(t)$ is bounded by r_{max} and at most one channel can be allocated to a given sensor, i.e., $\sum_{k \in \mathcal{K}} J_{n,k}(t) \leq 1$, the energy consumption is bounded by $P_n^{total}(t) \leq P_S r_{max} + P_T$. We use $P_{max} = P_S r_{max} + P_T$ to denote the upper bound of any sensor's energy consumption in a given time slot.

E. Energy Supply and Energy Queue Dynamics Model

Sensor n is equipped with a battery of limited capacity $\Omega_n, \forall n \in \mathcal{N}$. Because the battery capacity is the same for all sensors, we omitted the subscript n for simplicity. We use $E_n(t)$ to denote the energy queue length of sensor n. In time slot t, sensor n harvests energy $e_n(t)$ and consumes energy $P_n^{total}(t)$. Thus, the energy queue of sensor n evolves according to

$$E_n(t+1) = E_n(t) - P_n^{total}(t) + e_n(t). \tag{7}$$

In a given time slot t, the total energy consumption of sensor n must satisfy the following energy-availability constraint:

$$P_n^{total}(t) \leq E_n(t), \quad \forall n \in \mathcal{N}. \tag{8}$$

The energy harvesting process is characterized by the energy supply rate $\eta_n(t)$, which determines the amount of harvestable energy of sensor n in time slot t. The upper bound of $\eta_n(t)$ is denoted by $\eta_n \leq \eta_{max}$, $\forall n \in \mathcal{N}, t \in \mathcal{T}$. Furthermore, $\eta_n(t)$ randomly varies in an i.i.d fashion over slots. Notably, the exact distribution of $\eta_n(t)$ is not required, which is practically useful when knowledge of the EH process statistics is difficult to obtain. The harvested energy $e_n(t)$ is bounded by $\eta_n(t)$, i.e.,

$$0 \leq e_n(t) \leq \eta_n(t), \quad \forall n \in \mathcal{N}, \tag{9}$$

The total energy stored in the battery is limited by the battery capacity; thus, the following inequality must be satisfied in each time slot,

$$E_n(t) + e_n(t) \leq \Omega, \quad \forall n \in \mathcal{N}. \tag{10}$$

F. Data Transmission and Data Queue Dynamics Model

The amount of data that sensor n can transmit over channel k is determined by two factors: the availability of channel k, i.e., $S_k(t)$, and the channel capacity denoted by $\lambda_{n,k}(t)$. Considering the time-varying nature of channel fading, we assume that $\lambda_{n,k}(t)$ randomly varies over time slots in an i.i.d fashion and is bounded by $\lambda_{n,k}(t) \leq \lambda_{max}$, $\forall n \in \mathcal{N}, k \in \mathcal{K}$ as in [17].

The data transmission of the sensor on channel k fails if it collides with an active PU's transmission on channel k, i.e., $S_k(t) = 0$. Denote $x_n(t)$ as the data transmission rate of sensor n in time slot t. If channel k is allocated to sensor n, the data transmission rate $x_n(t)$ is bounded by

$$x_n(t) \leq \sum_{k \in \mathcal{K}} J_{n,k}(t) S_k(t) \lambda_{n,k}(t), \quad \forall n \in \mathcal{N}. \tag{11}$$

[1]The time is measured in unit size, thus the implicit multiplication by 1 slot is omitted when converting between power and energy [16] [17].

Let $Q_n(t)$ denote the data queue occupancy of sensor n and $\boldsymbol{Q(t)} = (Q_1(t), Q_2(t), \cdots, Q_N(t))$ represent a vector of length of data queues of all sensors. Note that $r_n(t)$ is the sampling rate, i.e., sensing rate, of sensor n in time slot t, and the dynamics of the data queue can be expressed as:

$$Q_n(t+1) = Q_n(t) - \sum_{k\in\mathcal{K}} J_{n,k}(t) S_k(t) x_n(t) + r_n(t), \quad (12)$$

where $J_{n,k}(t)x_n(t)$ captures the services process whereas $r_n(t)$ models the input process. This single-server queuing system is stable if the following network-stability constraint is satisfied [28]:

$$\lim_{T\to\infty} \frac{1}{T} \sum_{t=0}^{T-1} \sum_{n\in\mathcal{N}} \mathbb{E}[Q_n(t)] < \infty. \quad (13)$$

Constraint (13) implies that the data queues of all sensors have finite time-average occupancy.

In a given time slot, the n^{th} sensor can only transmit the available data in its queue; hence, the following data availability constraint must be satisfied in each time slot:

$$0 \le x_n(t) \le Q_n(t) \quad \forall n \in \mathcal{N}. \quad (14)$$

G. Optimization Problem Formulation

Based on the aforementioned models, we formulate the stochastic optimization problem. The objective is to maximize the time-average aggregate network utility of EHCRSNs subject to the constraints mentioned above. The time-average aggregate network utility problem can be written as

$$\bar{O} = \lim_{T\to\infty} \frac{1}{T} \sum_{t=0}^{T} -\mathbb{E}[O(t)], \quad (15)$$

where $O(t) = \sum_{n\in\mathcal{N}} U(r_n(t))$ denotes the network utility in a time slot. To simplify the presentation, we use $\boldsymbol{r}(t)$, $\boldsymbol{x}(t)$ and $\boldsymbol{e}(t)$ to denote the vectors of sampling rate $r_n(t)$, data transmission rate $x_n(t)$, and harvested energy $e_n(t)$ in time slot t, respectively. Additionaly, let $\boldsymbol{\Gamma}(t) \triangleq (\boldsymbol{r}(t), \boldsymbol{e}(t), \boldsymbol{x}(t), \mathbf{J}(t))$ represent the set of these variables in time slot t.

The network utility can be maximized by optimizing $\boldsymbol{\Gamma}(t)$ under the following utility maximization formulation,

$$\textbf{(UMP)} \ \max_{\boldsymbol{\Gamma}(t)} \bar{O}$$
$$\text{s.t. Eqs. (1) to (14)}$$

In the following section, we decompose **UMP** into a series of deterministic subproblems and relax the collision constraint (5), network-stability constraint (13), and energy-availability constraint (8) by employing Lyapunov optimization.

IV. Proposed Framework

With the above-described structure of **UMP**, it is challenging to design a low-complexity online algorithm to optimize the aggregate network utility without a priori knowledge of the energy harvesting, PU activity and channel fading statistics. The proposed framework is developed on the basis of Lyapunov optimization under which the **UMP** problem is decomposed into three deterministic subproblems. This approach facilitates achieving a close-to-optimal aggregate network utility and stability, and does not require a priori knowledge of the above-mentioned stochastic processes statistics [28].

A. Lyapunov Optimization

We define the network state in time slot t as $\boldsymbol{H}(t) \triangleq (\boldsymbol{Z(t)}, \boldsymbol{Q(t)}, \boldsymbol{E(t)}, \Theta(t))$ which captures the occupancy of collision queue, data queue, and energy queue and the conditions that affect the accuracy of channel availability estimation. Define a Lyapunov function, $L(t)$, as the sum of squares of backlogs in the collision and data queues, and the spare capacity in sensors' batteries as follows:

$$L(t) = \frac{1}{2}\sum_{k\in\mathcal{K}} (Z_k(t))^2 + \frac{1}{2}\sum_{n\in\mathcal{N}} (Q_n(t))^2 + \frac{1}{2}\sum_{n\in\mathcal{N}} \left(-\hat{E}_n(t)\right)^2, \quad (16)$$

where $\hat{E}_n(t) = \Omega - E_n(t)$ denotes the spare capacity of the n^{th} sensor battery. The Lyapunov function $L(t)$ can be considered a scalar measure of the congestion in $Z_k(t)$ and $Q_n(t)$, and the capacity availability in sensors' batteries. A small value of $L(t)$ indicates a low occupancy in the data and collision queues, as well as low spare capacity in energy queues $E_n(t)$, i.e., the batteries; the converse is also true. Additionally, we define the conditional Lyapunov drift as the one-slot difference of the Lyapunov function conditional on the network state, denoted by $\Delta(t) = \mathbb{E}[L(t+1) - L(t)|\boldsymbol{H}(t)]$. The expectation is taken over the randomness of energy harvesting, PU activity and channel fading, as well as the randomness in the energy management and channel allocation actions.

By minimizing $\Delta(t)$ in each time slot, the data queue $Q_n(t)$ and collision queue $Z_k(t)$ are pushed towards zero to stabilize the data queues and collision queues such that the network-stability constraint (13) and tolerable collision constraint (5) can be satisfied. Furthermore, the energy queues $E_n(t)$ are pushed towards their capacity Ω, such that sensors tend to recharge their batteries through energy harvesting. By carefully designing the value of Ω, the energy queues are guaranteed to have enough energy for data sensing and data transmission such that the energy-availability constraint (8) can be satisfied. The value of Ω is determined in Theorem 2 in Section V. Thus, constraints (5), (8) and (13) are satisfied.

At this point, the network utility to be maximized has not yet been incorporated. Therefore, we include a weighted version of the network utility into the Lyapunov drift, and instead of minimizing $\Delta(t)$, we minimize the following drift-minus-utility $\Delta_V(t)$ function:

$$\Delta_V(t) \triangleq \mathbb{E}[\Delta(t) - V O(t)|\boldsymbol{H}(t)], \quad (17)$$

where V is a non-negative importance weight that represents how much we emphasize on utility maximization [28]. In other words, instead of greedily minimizing $\Delta(t)$, we minimize $\Delta_V(t)$ to jointly stabilize the queues and optimize the weighted network utility $V O(t)$. With a sufficiently large value

of V, a close-to-optimal aggregate network utility can be achieved [29]. However, the data queues and energy queues become longer with a larger value of V, such that longer data queue buffers and battery capacities are required to support the EHCRSN. Thus, adjusting V allows a trade-off between the reduction of queue length and optimization of the network utility.

Considering that drift-minus-utility $\Delta_V(t)$ is a quadratic function of the queue lengths and variables in $\mathbf{\Gamma}(t)$, Lemma 1 derives the upper bound of $\Delta_V(t)$. The upper bound is a linear function of the queue length and the variables in $\mathbf{\Gamma}(t)$, which can be efficiently minimized.

Lemma 1: Given the variables in $\mathbf{\Gamma}(t)$, the value of $\Delta_V(t)$ is upper-bounded by:

$$\Delta_V(t) \leq B + \mathbb{E}[D_V(t)|\boldsymbol{H}(t)], \tag{18}$$

where the value of constant B is independent of V and can be expressed as

$$B = \frac{N}{2}\left[(\lambda_{max})^2 + (r_{max})^2 + (P_{max})^2 + (\eta_{max})^2\right] + \frac{1}{2}[K + \sum_{k\in\mathcal{K}}(\rho_k)^2] \tag{19}$$

and $D_V(t)$ is given in Eq. (20), as shown at the bottom of this page.

Proof: See Appendix A. ∎

Rather than minimizing the drift-minus-utility $\Delta_V(t)$ function, we try to minimize its the upper bound, i.e., the right-hand side (RHS) of Eq. (18). Furthermore, for a given network condition $\boldsymbol{H}(t)$, only $D_V(t)$ is relevant to the variables in $\mathbf{\Gamma}(t)$. Therefore, we minimize $D_V(t)$ by solving for the optimal sampling rate $\boldsymbol{r}(t)$, harvested energy $\boldsymbol{e}(t)$, data transmission rate $\boldsymbol{x}(t)$, and channel allocation $\mathbf{J}(t)$ in each time slot.

B. Framework Structure

Exploiting the linear structure of Eq. (20), $D_V(t)$ can be minimized after being decomposed it into three subproblems. In particular, the three subproblems are: battery management (**BM**), sampling rate control (**SRC**), and channel and data rate allocation (**CDRA**). Fig. 2 shows the three subproblems and the data flows among them. In the following, we treat each of the subproblems separately. The subproblems **BM** and **SRC** optimize the harvested energy $e_n(t)$ and sampling rate $r_n(t)$, respectively. Both **BM** and **SRC** require local information only available at the sensor, and they can be distributively solved at each sensor. However, **CDRA** is centrally solved at the sink because it requires information on the data queue occupancy $\boldsymbol{Q}(t)$, energy queue occupancy $\boldsymbol{E}(t)$, and channel collision queue occupancy $\boldsymbol{Z}(t)$ of all sensors. The sink gathers this information at the beginning of each time slot via the common control channel, as in [30]. In the following, each of the subproblems is solved separately.

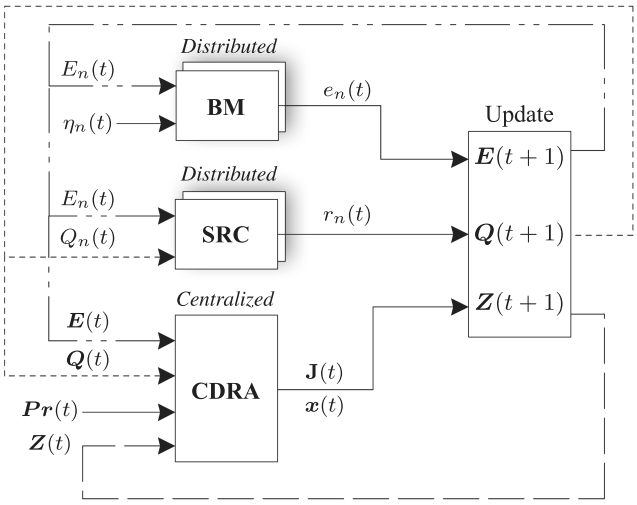

Fig. 2. Block diagram of the proposed framework showing the subproblems and the parameters exchanged among them.

- **Battery Management**
  Considering the first term on the RHS of (20) and the relevant constraints (9) and (10), we have the following optimization problem to solve for $e_n(t)$

$$\textbf{(BM)} \min_{e_n(t)} \; -\hat{E}_n(t)e_n(t) \quad \text{s.t.} \begin{cases} e_n(t) \leq \eta_n(t), \\ E_n(t) + e_n(t) \leq \Omega. \end{cases}$$

  If the battery is not full, i.e., $E_n(t) < \Omega$ and $\hat{E}_n(t) > 0$, the sensor should harvest as much energy as possible. Hence, if $E_n(t) < \Omega$, we have $e_n(t) = \min(\Omega - E_n(t), \eta_n(t))$; otherwise, set $e_n(t) = 0$.
- **Sampling Rate Control**
  Considering the second term on the RHS of (20) with constraint (1), we have the following optimization problem to optimize the sampling rate $r_n(t)$:

$$\textbf{(SRC)} \min_{r_n(t)} \; r_n(t)(Q_n(t) + P_S\hat{E}_n(t)) - VU(r_n(t)) \quad \text{s.t. } 0 \leq r_n(t) \leq r_{max}.$$

  The utility function $U(r_n(t))$ is concave; thus, the **SRC** problem is convex. Let the sampling rate $r_n^*(t)$ be the optimal solution to the **SRC** problem, based on the convex optimization theory [31], we have:

$$r_n^*(t) = \left[U'^{-1}\left(\frac{Q_n(t) + P_S\hat{E}_n(t)}{V}\right)\right]_0^{r_{max}} \tag{21}$$

$$D_V(t) = \sum_{n\in\mathcal{N}}\left[-\hat{E}_n(t)e_n(t)\right] + \sum_{n\in\mathcal{N}}\left[Q_n(t)r_n(t) + P_S r_n(t)\hat{E}_n(t) - VU(r_n(t))\right] + \sum_{n\in\mathcal{N}}\sum_{k\in\mathcal{K}} J_{n,k}(t)\left[Z_k(t)(1 - Pr_k(t)) - (Q_n(t)x_n(t)Pr_k(t) - P_T\hat{E}_n(t))\right] \tag{20}$$

where $[z]_a^b = \min(\max(z, a), b)$ and $U'^{-1}(\cdot)$ is the inverse of the first derivative of $U(\cdot)$.

- **Channel and Data Rate Allocation**
  Considering the third term on the RHS of (20) with constraints (2), (3), (4), (11) and (14), the problem of interest is determining the channel allocation matrix $\mathbf{J}(t)$ and data transmission rate $\boldsymbol{x}(t)$, which can be written as follows:

$$\textbf{(CDRA)} \min_{\mathbf{J}(t),\boldsymbol{x}(t)} \sum_{n\in\mathcal{N}}\sum_{k\in\mathcal{K}} J_{n,k}(t)[Z_k(t)(1-Pr_k(t)) - (Q_n(t)x_n(t)Pr_k(t) - P_T\hat{E}_n(t))]$$
$$\text{s.t. } (2)(3)(4)(11)(14).$$

CDRA optimizes the data transmission rate $\boldsymbol{x}(t)$ and channel allocation $\mathbf{J}(t)$; the former is a continuous variable and the latter is an integer variable which makes this subproblem a mixed integer problem. To facilitate the design of a tractable resource allocation solution, we transform **CDRA** into an integer problem by relaxing the constraints related to $\boldsymbol{x}(t)$, i.e., constraints (11) and (14). This is achieved over two steps. First, we adjust the data queue length and modify the objective function of **CDRA**; we refer to it hereafter as the modified **CDRA (m-CDRA)**. We show that the objective function of **m-CDRA** is minimized if sensors transmit data at full capacity on their assigned channels. Second, we replace the continuous variable $x_n(t)$ by the channel capacity $\lambda_{n,k}(t)$ in the objective function of **m-CDRA**. Thus, we can relax constraints (11) and (14) and transform the **m-CDRA** problem into a Channel Allocation **(CA)** problem, which is a one-to-one matching problem. These steps are detailed in the following:

1) Define the adjusted length of the data queue as

$$\hat{Q}_n(t) = [Q_n(t) - \lambda_{max}]^+. \tag{22}$$

After replacing $Q_n(t)$ by $\hat{Q}_n(t)$ in the objective function of the **CDRA** problem, we rewrite the objective function as

$$\sum_{n\in\mathcal{N}}\sum_{k\in\mathcal{K}} J_{n,k}(t)M_{n,k}(t), \tag{23}$$

where $M_{n,k}(t) = [Z_k(t)(1-Pr_k(t)) - (\hat{Q}_n(t)x_n(t)Pr_k(t) - P_T\hat{E}_n(t))]$. Instead of solving the original **CDRA**, we solve the modified **m-CDRA** with Eq. (23) as the objective function to find a suboptimal solution for the original **CDRA**. Suppose that $\mathbf{J}^*(t)$ and $\boldsymbol{x}^*(t)$ are the optimal solutions for the **m-CDRA**; in the following lemmas, we show that a channel k is assigned to sensor n if and only if it has a sufficient amount of data to transmit and it transmits it at full channel capacity.

Lemma 2: For a channel k to be assigned to sensor n, i.e., $\sum_{k\in\mathcal{K}} J^*_{n,k}(t) = 1$, the following must be satisfied

$$Q_n(t) > \lambda_{max}. \tag{24}$$

Proof: See Appendix B. ∎

*Lemma 3: If any channel is assigned to the n^{th} sensor in the t^{th} time under the modified **m-CDRA**, i.e., $\sum_{k\in\mathcal{K}} J^*_{n,k}(t) = 1$, then we have*

$$x^*_n(t) = \sum_{k\in\mathcal{K}} J^*_{n,k}(t)\lambda_{n,k}(t), \tag{25}$$

otherwise, $x^*_n(t) = 0$.

Proof: See Appendix C. ∎

2) Lemma 3 shows that the sensor must fully utilize the assigned channel to optimally solve **m-CDRA**. Therefore, we can replace the transmission rate $x_n(t)$ by channel capacity $\lambda_{n,k}(t)$ in Eq. (23) and, thus, relax the channel capacity constraint (11) and data-availability constraint (14). The modified **m-CDRA** is transformed into a **CA** problem as follows:

$$\textbf{(CA)} \min_{\mathbf{J}(t)} \sum_{n,k} J_{n,k}(t)\left[Z_k(t)(1-Pr_k(t)) - \left(\hat{Q}_n(t)\lambda_{n,k}(t)Pr_k(t) - P_T\hat{E}_n(t)\right)\right]$$
$$\text{s.t. } (2)(3)(4).$$

CA can be mapped to a one-to-one matching problem. Furthermore, due to the limited number of transceivers on the sink, i.e., $L \leq K$, a maximum of L channels can be allocated to sensors in a given time slot. Meanwhile, if $L < K$, i.e., not all channels can be allocated to the sensors, **CA** is an unbalanced matching problem, which can be solved by the adaptive Hungarian algorithm proposed in [32]. The complexity of the algorithm increases linearly with the number of sensors.

C. Utility-Optimal Resource Management and Allocation Algorithm (UoRMA)

In this subsection, we present the UoRMA algorithm in Algorithm 1. The UoRMA algorithm achieves the optimal harvested energy $\boldsymbol{e}^*(t)$, sampling rate $\boldsymbol{r}^*(t)$, data transmission rate $\boldsymbol{x}^*(t)$, and channel allocation $\mathbf{J}^*(t)$ by solving **BM**, **SRC** and **CDRA**, respectively. Moreover, the occupancy of data queues $\boldsymbol{Q}(t)$, energy queues $\boldsymbol{E}(t)$ and collision queues $\boldsymbol{Z}(t)$ are updated according to their respective queue dynamics.

Both the **BM** and **SRC** problems have closed-form solutions, and can be distributively solved at each sensor. Thus, their complexity is negligible. The complexity of Algorithm 1 is dominated by solving the **CA** problem in step 8 with time complexity of $O(NKL+L^2\log(\min(N, K)))$ [32]. Therefore, the complexity of UoRAM increases linearly with the number of sensors N. Notably, the complexity of algorithms designed based on Markov Decision Process (MDP) increases exponentially with N [33]. Comparing to the MDP-based algorithms, UoRMA is more computationally efficient in addition to being scalable for densely deployed sensor networks.

V. Performance Analysis

In this section, we analyze the stability and performance of the proposed UoRMA algorithm. Theorem 1 proves the stability of EHCRSNs operating under the UoRMA algorithm

Algorithm 1: Proposed UoRMA Algoritm

Data: $\boldsymbol{Z}(t)$, $\boldsymbol{Q}(t)$, $\boldsymbol{E}(t)$, $\boldsymbol{Pr}(t)$, $\eta_n(t), \forall n \in \mathcal{N}$, $\lambda_{n,k}(t), \forall n \in \mathcal{N}, \forall k \in \mathcal{K}$.

Result: $\boldsymbol{r}^*(t)$, $\boldsymbol{e}^*(t)$, $\boldsymbol{x}^*(t)$, $\mathbf{J}^*(t)$, $\boldsymbol{Z}(t+1)$, $\boldsymbol{Q}(t+1)$, $\boldsymbol{E}(t+1)$.

/* Battery Management */

foreach $n \in \mathcal{N}$ **do**
  if $E_n(t) < \Omega$ **then**
    $e_n^*(t) = \min(\Omega - E_n(t), \eta_n(t))$;
  else
    $e_n^*(t) = 0$;

/* Sampling Rate Control */

foreach $n \in \mathcal{N}$ **do**
  Compute $r_n^*(t)$ based on Eq. (21);

/* Channel and Data Rate Allocation */

Solve **CA** problem and set $\mathbf{J}^*(t)$;

foreach $n \in \mathcal{N}$ **do**
  if $\sum_{k\in\mathcal{K}} J_{n,k}^*(t) == 1$ **then**
    $x_n^*(t) = \sum_{k\in\mathcal{K}} J_{n,k}^*(t)\lambda_{n,k}(t)$;
  else
    $x_n^*(t) = 0$;

/* Update the queue lengths */

foreach $n \in \mathcal{N}$ **do**
  Compute $Q_n(t+1)$ based on Eq. (12);
  Compute $E_n(t+1)$ based on Eq. (7);

foreach $k \in \mathcal{K}$ **do**
  Compute $Z_k(t+1)$ based on Eq. (6);

by deriving upper bounds on the length of the data queues and collision queues. Then, we derive the required battery capacity to support the operation of the EHCRSN in Theorem 2. Theorem 3 evaluates the gap between the network's aggregate utility obtained by UoRMA and the optimal solution to demonstrate the optimality of UoRMA.

A. Upper Bounds on Data Queues and Collision Queues

We derive the upper bounds on the occupancies of queues and collision queues in Theorem 1. The existence of the bounds guarantees satisfying the data and collision queue stability constraints (13) and (5).

Theorem 1: For a non-negative parameter V, $P_k(t) \leq 1-\varepsilon$, $\forall k, t$, and an initialization of the collision queue and data queue satisfying $0 \leq Z_k(0) \leq Z_{max}$, $\forall k \in \mathcal{K}$ and $0 \leq Q_n(0) \leq Q_{max}$, $\forall n \in \mathcal{N}$, where the upper bounds are given by

$$Q_{max} = \zeta_U V + r_{max},$$
$$Z_{max} = \frac{Q_{max}\lambda_{max}(1-\varepsilon)}{\varepsilon} + 1,$$

we have

$$0 \leq Q_n(t) \leq Q_{max}, \quad \forall n \in \mathcal{N}, \tag{26}$$
$$0 \leq Z_k(t) \leq Z_{max}, \quad \forall k \in \mathcal{K}. \tag{27}$$

Proof: See Appendix D. ∎

As we can see from Eqs. (26) and (27), both the upper bounds of data queues and collision queues increase linearly with the weight V. Since a larger V can bring higher network utility, the linear increase of upper bound on data queues indicates that a longer data buffer is required at each sensor to achieve better network performance. Furthermore, the increase of upper bound on collision queues also indicates that the PUs may experience more collisions from the EHCRSN. However, the collision constraint (5) can still be satisfied due to the existence of the upper bound on collision queues.

B. Required Battery Capacity Ω

In Theorem 2, we determine the required battery capacity Ω in such a way that the sensor does not sense or transmit any data if the available energy is less than the maximum energy consumption of each sensor, i.e., $E_n(t) \leq P_{max}$. Therefore, the energy-availability constraint (8) becomes implicit.

Theorem 2: Under the proposed framework and with a battery capacity Ω given by

$$\Omega = \max\left(\frac{V\zeta_U}{P_S} + P_{max}, \frac{Q_{max}\lambda_{max}}{P_T} + P_{max}\right), \quad \forall n \in \mathcal{N}, \tag{28}$$

sensor n does not sense data or is not allocated a channel, i.e., $r_n(t) = 0$ and $\sum_{k\in\mathcal{K}} J_{n,k}(t) = 0$, if the energy queue length in a given time slot is less than the upper bound of the sensor's energy consumption, i.e., $E_n(t) < P_{max}$.

Proof: See Appendix E. ∎

The required battery capacity in (28) is determined by both the transmission power P_T and the sensing/processing power P_S because both data arrival and departure consume energy in EHCRSNs.

C. Optimality of the UoRMA Algorithm

In Theorem 3, the optimality of the UoRMA algorithm is analyzed.

Theorem 3: Suppose that the optimal network utility that can be achieved by an exact and optimal algorithm is O^* and that the network utility $\bar{O}$ achieved by the UoRMA algorithm satisfies:

$$\bar{O} \geq O^* - \frac{\tilde{B}}{V} \tag{29}$$

where $\tilde{B} = B + NK(\lambda_{max})^2$.

Proof: See Appendix F. ∎

If we do not transform **CDRA** to **CA**, then the gap between the solution obtained by the proposed algorithm and the optimal solution can be determined by B/V [28], where B is the constant defined in Lemma 1. Thus, the performance loss caused by the transformation is shown in $\tilde{B}$, which is larger than B. However, by Theorem 3, we see that the UoRMA algorithm can achieve an aggregate network utility within $O(1/V)$ of the optimal utility without a priori knowledge of the statistics of the stochastic processes such as channel fading, PU activities, and energy harvesting.

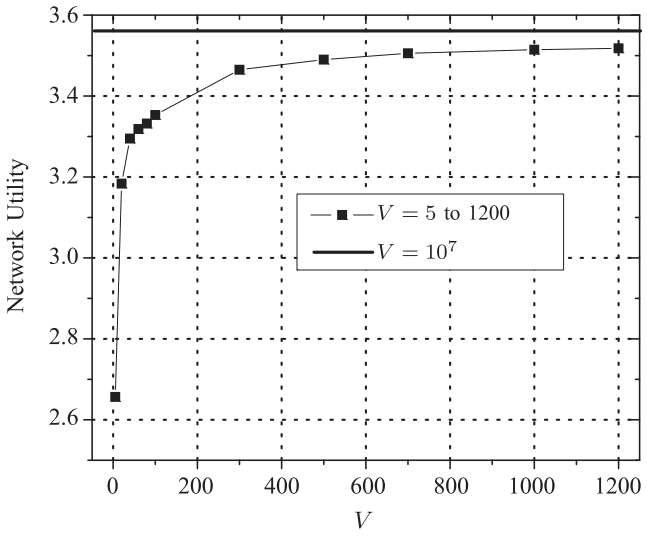

Fig. 3. Network utility for the range of V = [5, 20, 40, 60, 80, 100, 300, 500, 700, 1000, 1200].

VI. Simulation Results

In this section, we provide simulation results to evaluate the performance of the UoRMA algorithm in EHCRSNs. The simulated EHCRSN is randomly deployed in a circular area with a radius of 30 m and consists of $N = 15$ sensors. The sink has $L = 3$ transceivers, and is located at the center of this circular area. Similar to [17] and [16], we define a concave utility function $U(r_n(t)) = \log(1 + r_n(t))$, $\forall n \in \mathcal{N}$ and, $\zeta_U = 1$. The EHCRSN operates on $K = 4$ licensed channels. The energy consumption rate of data sensing $P_S = 0.1$, and the maximum sampling rate $r_{max} = 5$. The maximum energy supply rate is set to $\eta_{max} = 2$, while the energy supply rate $\eta_n(t), \forall n \in \mathcal{N}$ is uniformly distributed in $[0, \eta_{max}]$.

The PU on channel k, $\forall k \in \mathcal{K}$, is inactive with probability 0.4 in each time slot. Given that PU on channel k is inactive in time slot t, the channel access probability $Pr_k(t) = 0.9$; otherwise, $Pr_k(t) = 0.1$, i.e., the misdetection and false alarm probabilities are 0.1 [14]. The tolerable collision rate ρ_k, $\forall k \in \mathcal{K}$ is set to 0.05 [21].

The channel capacity $\lambda_{n,k}(t) = \log(1 + \frac{P_T h_{n,k}(t)}{d_n^4 N_0})$ where d_n denotes the distance between sensor n and the sink, noise power $N_0 = 10^{-5}$, and the transmission power $P_T = 1$. Furthermore, the channel fading coefficients $h_{n,k}(t)$ are uniformly distributed between $(0.9, 1.1)$ and i.i.d across time slots; i.e., the values 0.9 and 1.1 model stable channel conditions [16]. The upper bound of the channel capacity is $\lambda_{max} = 2$ [16]. The energy queue is initialized as in Eq. (28) in time slot $t = 0$, whereas the data queue and collision queue are empty at $t = 0$. The length of the simulation is set to $|\mathcal{T}| = 2 \times 10^4$.

A. Network Utility and Queue Dynamics

In Fig. 3, we evaluate the network utility versus the value of V ranging from 5 to 1200. The figure shows that the network utility increases with increase of V. However, the rate at which the network utility increases decreases with larger V. This is expected because the network utility is a concave function of V, as shown in Eq. (42). We take a large value of V to illustrate the optimal network utility ($V = 10^7$ in our setting). We compare the network utility obtained by V ranging from 5 to 1200 to the network utility obtained by $V = 10^7$. As shown in the figure, the increase of network utility from $V = 1200$ to $V = 10^7$ is quite limited in comparison to the increasing from $V = 5$ to $V = 1200$. Therefore, the network utility achieved when $V = 1200$ is close to the value of the optimal network utility.

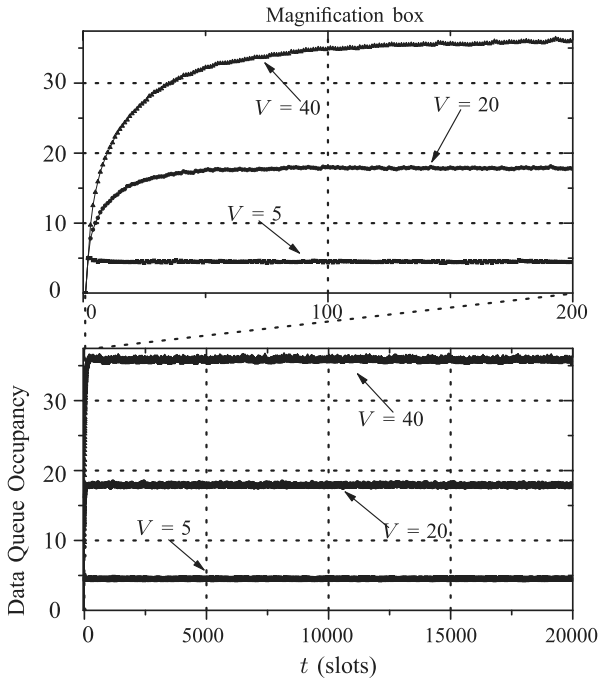

Fig. 4. Data queue occupancy for different values of V.

Fig. 4 shows the data queue occupancy over 20,000 slots for different values of V. The time-average lengths of data queues increase with the value of V. Furthermore, it can be seen that the lengths of data queues converge quickly to the time-average value. This is because the battery is fully charged at $t = 0$, such that sensors can sense data at $t = 1$.

Fig. 5 shows the collision queue occupancy for different values of V. Similar to the data queue dynamics shown in Fig. 4, the time-average lengths of the collision queues increase with larger values of V, and the lengths of the collision queues fluctuate around a time-average value after the convergence. When the collision queue is small, the UoRMA algorithm tends to allocate the channel to sensors for data transmission. If the allocated channel is actually occupied by PUs, the collision queue increases back to the time-average value. Therefore, the collision queue length affects the dynamics of the queue's fluctuation. In addition, sensors' data queues and energy queues lengths also affect the dynamics of the fluctuation, because the UoRMA algorithm tends to allocate channels to the sensors with long data queues and small spare capacity in the energy queues.

B. Impact of Parameter Variations

In the following, we evaluate the impacts of various system parameters on the network utility. Assuming all channels have

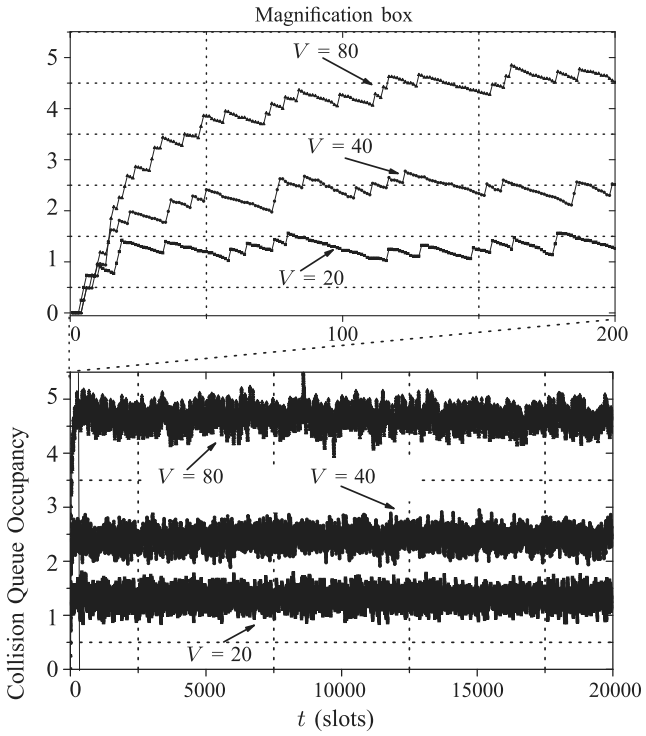

Fig. 5. Collision queue occupancy for different values of V.

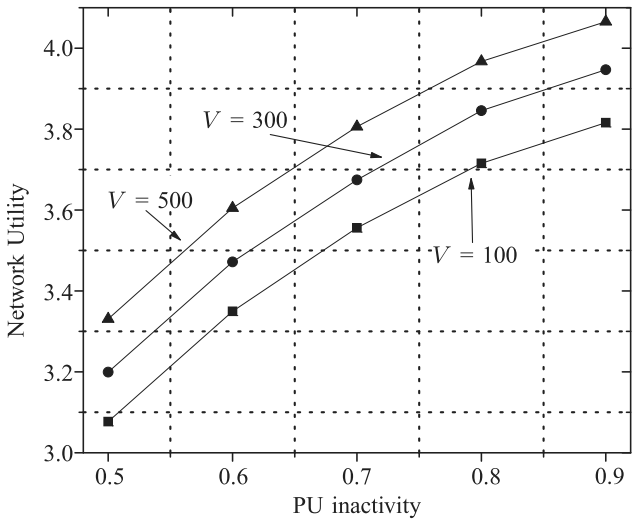

Fig. 6. Network utility versus PU inactivity probability.

the same PU inactivity probability ranging from 0.5 to 0.9, we first verify the network utility in Fig. 6. The figure shows that the network utility increases with increase in the PU inactivity probability. At the same time, the rate of increase in the network utility decays with higher PU inactivity probability due to the limited energy supply rate.

Fig. 7 shows the network utility versus maximum available energy supply η_{max} ranging from 1 to 5. The network utility monotonically increases with increasing η_{max} because more energy can be used to sense and transmit data. However, similar to Fig. 6, the growth rate of the network utility decays with higher η_{max}. This indicates that, given sufficient energy

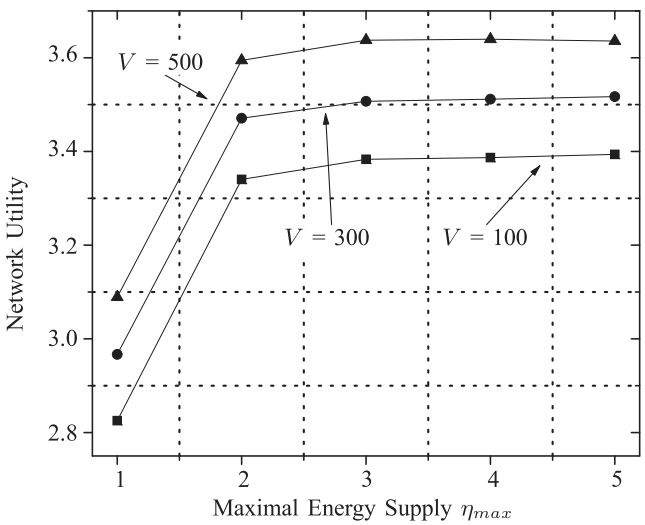

Fig. 7. Network utility versus maximal energy supply η_{max}.

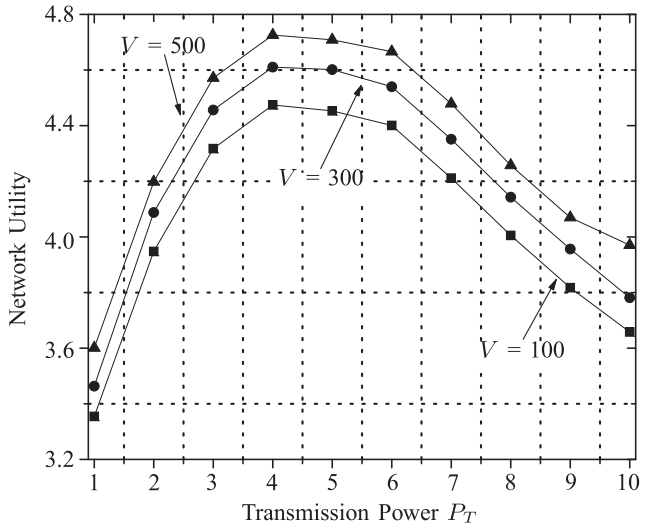

Fig. 8. Network utility versus transmission power P_T.

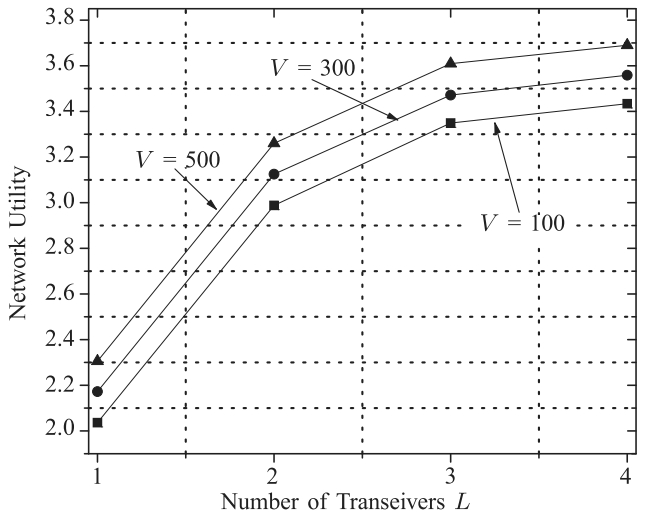

Fig. 9. Network utility versus number of transceivers L.

supply, the network utility is bounded by the channel availability which also limits the sensors' chance of transmitting data.

Fig. 8 shows the network utility versus transmission power P_T. As shown in the figure, there exists an optimal value of P_T that maximizes the network utility. In our simulations, the optimal value of P_T is 4. If P_T is smaller than this optimal value, the available channels are underutilized which leads to lower network utility. However, if P_T is larger than this optimal value, sensors need more time to harvest energy for data transmission, which also reduces the network utility.

Fig. 9 shows the network utility versus the number of transceivers that are mounted on the sink, L. Since the sink can support more concurrent data transmission with more transceivers, the network utility increases with L when $L \leq K$, i.e., number of transceivers is not larger than the number of licensed channels.

VII. Conclusion

In this paper, we have developed an aggregate network utility optimization framework to facilitate the design of an online and low-complexity algorithm for managing and allocating the resources of EHCRSNs. The proposed framework captures and optimizes stochastic energy harvesting and consumption processes, as well as stochastic spectrum utilization and access processes. We employ Lyapunov optimization to decompose the problem into three sub-problems that are easier to solve, battery management, sampling rate control, and data rate and channel allocation. The solutions proposed to solve the three problems constitute the proposed utility-optimal resource management and allocation (UoRMA) algorithm. The optimality gap and bounds on data and energy queues are derived. The proposed algorithm achieves a close-to-optimal aggregate network utility while ensuring bounded energy and date queues. Simulations verify the optimality and stability of EHCRSN when operating under UoRMA algorithm. The outcomes of this work can be used to guide the design of practical EHCRSNs by guaranteeing PU protection and sensors sustainability.

For future work, we plan to investigate stochastic energy management and channel allocation for EHCRSNs to collect delay-sensitive data. In addition, the adaptive transmission power of sensors will be considered.

Appendix A
Proof of Lemma 1

By squaring both sides of Eq. (6), we have Eq. (30). Similarly, we have Eq. (31) from Eq. (12), and Eq. (32) from Eq. (7), respectively. Substituting $\mathbb{E}[C_k(t)|\Theta(t)] = \sum_{k\in\mathcal{K}} J_{n,k}(t) Pr_k(t)$ and $\mathbb{E}[1 - S_k(t)|\Theta(t)] = 1 - Pr_k(t)$ into Eq. (31) and rearranging the equation, we have Eq. (20).

$$\begin{aligned}
&\frac{1}{2}\left[(Z_k(t+1))^2 - (Z_k(t))^2\right] \\
&\leq \frac{\left[(C_k(t))^2 + (\rho_k 1_k)^2 + 2Z_k(t)(C_k(t) - \rho_k 1_k)\right]}{2} \\
&\leq \frac{1 + (\rho_k)^2}{2} + Z_k(t)(C_k(t) - \rho_k 1_k). \qquad (30)
\end{aligned}$$

$$\begin{aligned}
&\frac{1}{2}\left[(Q_n(t+1))^2 - (Q_n(t))^2\right] \\
&\leq \frac{1}{2}\left[\left(\sum_{k\in\mathcal{K}} J_{n,k}(t)x_n(t)S_k(t)\right)^2\right. \\
&\quad \left. + (r_n(t))^2 + 2Q_n(t)\left(r_n(t) - \sum_{k\in\mathcal{K}} J_{n,k}(t)x_n(t)S_k(t)\right)\right] \\
&\leq \frac{(\lambda_{max})^2 + (r_{max})^2}{2} \\
&\quad + Q_n(t)\left(r_n(t) - \sum_{k\in\mathcal{K}} J_{n,k}(t)x_n(t)S_k(t)\right) \qquad (31)
\end{aligned}$$

$$\begin{aligned}
&\frac{1}{2}\left[(E_n(t+1) - \Omega)^2 - (E_n(t) - \Omega)^2\right] \\
&\leq \frac{\left[(P_n^{total}(t))^2 + (e_n(t))^2 - 2\hat{E}_n(t)\left(e_n(t) - P_n^{total}(t)\right)\right]}{2} \\
&\leq \frac{(P_{max})^2 + (\eta_{max})^2}{2} - 2\hat{E}_n(t)\left(e_n(t) - P_n^{total}(t)\right) \qquad (32)
\end{aligned}$$

Appendix B
Proof of Lemma 2

First, we prove that if there is any channel assigned to sensor n, its adjusted queue length $\hat{Q}_n(t) > 0$. Suppose that channel k is assigned to sensor n, i.e., $J^*_{n,k}(t) = 1$, it is obvious that $M_{n,k}(t) = Z_k(t)(1 - Pr_k(t)) + P_T\hat{E}_n(t) - \hat{Q}_n(t)x_n(t)Pr_k(t) < 0$. Since $Z_k(t)(1 - Pr_k(t)) \geq 0$, $P_T\hat{E}_n(t) \geq 0$, and $x_n(t)Pr_k(t) \geq 0$, the adjusted data queue length becomes larger than zero, i.e., $\hat{Q}_n(t) > 0$.

Then, we prove that if $\hat{Q}_n(t) > 0$, then the queue length $Q_n(t) > \lambda_{max}$. Recalling that $\hat{Q}_n(t) = \max(Q_n(t) - \lambda_{max}, 0)$, $\hat{Q}_n(t) > 0$ implies that $Q_n(t) - \lambda_{max} > 0$, i.e., the data queue length $Q_n(t)$ is larger than the maximum channel capacity λ_{max}.

Appendix C
Proof of Lemma 3

We first consider the condition that sensor n is not assigned with any channel, thus $J_{n,k} = 0$, $\forall k \in \mathcal{K}$. According to constraint (11) and $x_n(t) \geq 0$, we have $x^*_n(t) = 0$.

Next, we prove that $x^*_n(t) = \sum_{k\in\mathcal{K}} J^*_{n,k}(t)\lambda_{n,k}(t)$ is the optimal solution for the condition that $\sum_{k\in\mathcal{K}} J^*_{n,k}(t) = 1$. We use k_n to denote the channel assignment to sensor n, i.e., $J^*_{n,k_n} = 1$. Since M_{n,k_n} is inversely correlated with the value of $x_n(t)$, the value of $x_n(t)$ should be as large as possible to minimize M_{n,k_n}. The value of $x_n(t)$ is bounded by constraints (11) and (14), i.e., the channel capacity and data queue length $Q_n(t)$. According to Lemma 2, we can see that the data queue length $Q_n(t)$ must exceed the maximum channel capacity ($Q_n(t) \geq \lambda_{max}$) if $\sum_{k\in\mathcal{K}} J^*_{n,k}(t) = 1$. Therefore, $x_n(t)$ is only bounded by channel capacity constraint in (11). Then we have the optimal $x_n(t)$ to be $x^*_n(t) = \lambda_{n,k_n}(t)$.

Appendix D
Proof of Theorem 1

At $t = 0$, Eq. (26) holds. In the following, we prove Eq. (26) by inductions. We first assume that Eq. (26) holds in time slot t, and then prove that it holds in $t + 1$.

1) If sensor n does not sense any data, then we have $Q_n(t+1) \le Q_n(t) \le \zeta_U V + r_{max}$;
2) If sensor n collects data with sampling rate $r_n^*(t)$, given in Eq. (21), then we have $VU'(r_n^*(t)) = Q_n(t) - P_S(E_n(t) - \Omega)$ and $Q_n(t) \le VU'(r_n^*(t))$. Since $U'(r_n^*(t)) \le \zeta_U$, $\forall r_n(t)$ where ζ_U denotes the upper bound of the first-order derivative of $U(r_n(t))$, $\forall r_n(t)$, we have $Q_n(t) \le V\zeta_U$. Furthermore, since $r_n^*(t) \le r_{max}$, we have $Q_n(t+1) \le Q_n(t) + r_{max} \le V\zeta_U + r_{max}$.

Summarily, we have $Q_n(t+1) \le V\zeta_U + r_{max}$. This completes the proof of Eq. (26).

Then we prove Eq. (27) by inductions. At $t = 0$, the collision queue is initialized as an empty queue. We prove that if Eq. (27) holds in time slot t, it will hold in $t+1$.

1) If $P_k(t) = 1$, then no collision can happen, such that $Z_k(t+1) \le Z_k(t) \le Z_{max}$.
2) If $P_k(t) \le 1 - \varepsilon$, and $Z_k(t) \le Z_{max} - 1$, then we have $Z_k(t+1) \le Z_k(t) + 1 \le Z_{max}$.
3) If $P_k(t) \le 1 - \varepsilon$, and $Z_k(t) > Z_{max} - 1$, then we have $Z_k(t)(1 - Pr_k(t)) - P_T(E_n(t) - \Omega) - Q_n(t)x_n(t)Pr_k(t)) \ge 0$, so channel k can not be allocated to any sensor in problem **CA**. This would yield $C_k(t) = 0$. Therefore, we have $Z_k(t+1) \le Z_k(t) \le Z_{max}$.

Summarily, we have $Z_k(t+1) \le Z_{max}$. This completes the proof of Eq. (27).

Appendix E
Proof of Theorem 2

We first derive an expression for Ω in such a way that sensor n does not sense data, i.e., $r_n(t) = 0$ if $E_n(t) < P_{max}$. The sampling rate $r_n(t)$ is determined by Eq. (21). The utility function $U(r_n(t))$ is concave; therefore, $U'^{-1}(r_n(t))$ and $r_n(t)$ are inversely proportional. Based on Eq. (21), sensor n does not sense any data, i.e., the sampling rate is $r_n(t) = 0$, if

$$\frac{Q_n(t) + P_S\hat{E}_n(t)}{V} \ge \zeta_U \ge U'(0). \tag{33}$$

Recall that $\hat{E}_n(t) = \Omega - E_n(t)$ and rearrange Eq. (33) to $\Omega \ge \frac{V\zeta_U}{P_S} + E_n(t)$. To satisfy that the sensor cannot sense any data when $E_n(t) < P_{max}$, Ω can be set as follows $\Omega \ge \frac{V\zeta_U}{P_S} + P_{max}$.

Then we derive the value of Ω in such a way that no channel can be allocated to sensor n, i.e., $\sum_{k\in\mathcal{K}} J_{n,k}(t) = 0$, if $E_n(t) < P_{max}$. As we can see from the objective function of **CA**, no channel can be allocated to n if

$$Z_k(t)(1 - Pr_k(t)) + P_T\hat{E}_n(t) - \hat{Q}_n(t)\lambda_{n,k}(t)Pr_k(t) \ge 0. \tag{34}$$

Rearrange equation (34) to

$$\Omega \ge \frac{\hat{Q}_n(t)\lambda_{n,k}(t)Pr_k(t) - Z_k(t)(1 - Pr_k(t))}{P_T} + E_n(t). \tag{35}$$

Since $Pr_k \le 1$, $\hat{Q}_n(t) \le Q_{max}$, $Z_k(t) \ge 0$ and $\lambda_{n,k}(t) \le \lambda_{max}$, we can change the RHS of Eq. (35) to $Q_{max}\lambda_{max}/P_T + E_n(t)$. To guarantee that no channel can be allocated to sensor n if $E_n(t) < P_{max}$, Ω can be set to $\Omega \ge \frac{Q_{max}\lambda_{max}}{P_T} + P_{max}$. Theorem 2 is thus proved.

Appendix F
Proof of Theorem 3

We prove the theorem by comparing the Lyapunov drift with a stationary and randomized algorithm denoted by Π. We introduce superscript Π to variables $\boldsymbol{r}^\Pi(t)$, $\boldsymbol{e}^\Pi(t)$, $\mathbf{J}^\Pi(t)$, and $P_n^{total,\Pi}(t)$ to indicate that these variables are generated under algorithm Π. Since all of the PU activities, channel condition, and EH process change in i.i.d manners across the time slots, according to [28, Th. 4.5], algorithm Π can yield

$$\mathbb{E}\left[\sum_{n\in\mathcal{N}} U(r_n^\Pi(t))\right] \le O^* + \delta, \tag{36}$$

$$\left|\mathbb{E}\left[\sum_{k\in\mathcal{K}}\left(C_k^\Pi(t) - \rho_k(1 - S_k(t))\right)\right]\right| \le \varrho_1\delta, \tag{37}$$

$$\left|\mathbb{E}\left[\sum_{n\in\mathcal{N}}\left(r_n(t) - \sum_{k\in\mathcal{K}} J_{n,k}^\Pi(t)x_n(t)S_k(t)\right)\right]\right| \le \varrho_2\delta, \tag{38}$$

$$\left|\mathbb{E}\left[\sum_{n\in\mathcal{N}}\left(e_n^\Pi(t) - P_n^{total,\Pi}(t)\right)\right]\right| \le \varrho_3\delta, \tag{39}$$

where $\delta > 0$ can be arbitrarily small, and ϱ_1, ϱ_2 and ϱ_3 are constant scalars.

In each time slot, the UoRAM algorithm minimizes the right hand side of the Lyapunov drift in Eq. (40), as shown at the bottom of this page.

The proof of Eq. (40) can be obtained by [17, Th. 2]. Note that $\Delta(t) - V\mathbb{E}[\sum_{n\in\mathcal{N}} U(r_n(t))] \le \tilde{B} + \mathbb{E}[\tilde{D}_V(t)|\boldsymbol{H}(t)]$, where $\tilde{B} = B + NK(\lambda_{max})^2$ is a constant w.r.t. the variables, we can have the following inequality:

$$\begin{aligned}
&\Delta(t) - V\mathbb{E}\left[\sum_{n\in\mathcal{N}} U(r_n(t))\right] \\
&\le \tilde{B} + \mathbb{E}\left[\tilde{D}_V^{UoRMA}(t)|\boldsymbol{H}(t)\right] \\
&\le \tilde{B} + \mathbb{E}[\tilde{D}_V^\Pi(t)] \\
&\le \tilde{B} + (\varrho_1 + \varrho_2 + \varrho_3)\delta + O^* + \delta,
\end{aligned} \tag{41}$$

$$\begin{aligned}
\tilde{D}_V(t) = &\sum_{k\in\mathcal{K}} Z_k(t)\left(C_k(t) - \rho_k(1 - S_k(t))\right) - \sum_{n\in\mathcal{N}} \hat{E}_n(t)\left(e_n(t) - P_n^{total,\Pi}(t)\right) \\
&- \sum_{n\in\mathcal{N}}\left(VU(r_n(t)) - Q_n(t)r_n(t)\right) - \sum_{n\in\mathcal{N}}\sum_{k\in\mathcal{K}} J_{n,k}(t)x_n(t)S_k(t)\hat{Q}_n(t),
\end{aligned} \tag{40}$$

where $\tilde{D}_V^{UoRMA}(t)$ and $\tilde{D}_V^{\Pi}(t)$ denote the value of $\tilde{D}_V(t)$ obtained under UoRMA algorithm and algorithm Π, respectively. By setting δ to zero, we can have

$$\Delta(t) - V\mathbb{E}\left[\sum_{n\in\mathcal{N}} U(r_n(t))\right] \leq O^* + \tilde{B}. \tag{42}$$

Taking the expectation on both sides of (42), summing up the equations for $t \in \mathcal{T}$, dividing by T and letting $T \to \infty$, we have $\bar{O} \geq O^* - \tilde{B}/V$. Theorem 2 is thus proved.

REFERENCES

[1] S. He, J. Chen, F. Jiang, D. K. Y. Yau, G. Xing, and Y. Sun, "Energy provisioning in wireless rechargeable sensor networks," *IEEE Trans. Mobile Comput.*, vol. 12, no. 10, pp. 1931–1942, Oct. 2013.

[2] Z. Su, Q. Xu, and Q. Qi, "Big data in mobile social networks: A QoE-oriented framework," *IEEE Netw.*, vol. 30, no. 1, pp. 52–57, Jan./Feb. 2016.

[3] M. Gorlatova, J. Sarik, G. Grebla, M. Cong, I. Kymissis, and G. Zussman, "Movers and shakers: Kinetic energy harvesting for the Internet of things," *IEEE J. Sel. Areas Commun.*, vol. 33, no. 8, pp. 1624–1639, Aug. 2015.

[4] S. Sudevalayam and P. Kulkarni, "Energy harvesting sensor nodes: Survey and implications," *IEEE Commun. Surveys Tuts.*, vol. 13, no. 3, pp. 443–461, Sep. 2011.

[5] I. F. Akyildiz, W.-Y. Lee, M. C. Vuran, and S. Mohanty, "Next generation/dynamic spectrum access/cognitive radio wireless networks: A survey," *Comput. Netw.*, vol. 50, no. 13, pp. 2127–2159, 2006.

[6] J. Ren, Y. Zhang, R. Deng, N. Zhang, D. Zhang, and X. Shen, "Joint channel access and sampling rate control in energy harvesting cognitive radio sensor networks," *IEEE Trans. Emerg. Topics Comput.*, to be published, doi : 10.1109/TETC.2016.2555806.

[7] (Oct. 2016). *Avoiding RF Interference Between WiFi and ZigBee*. [Online]. Available: http://www.mobiusconsulting.com/papers/ZigBeeandWiFiInterference.pdf

[8] P. Phunchongharn, E. Hossain, D. Niyato, and S. Camorlinga, "A cognitive radio system for e-health applications in a hospital environment," *IEEE Wireless Commun.*, vol. 17, no. 1, pp. 20–28, Feb. 2010.

[9] E. Ibarra, A. Antonopoulos, E. Kartsakli, J. J. P. C. Rodrigues, and C. Verikoukis, "QoS-aware energy management in body sensor nodes powered by human energy harvesting," *IEEE Sensors J.*, vol. 16, no. 2, pp. 542–549, Jan. 2016.

[10] F. Sánchez-Rosario *et al.*, "A low consumption real time environmental monitoring system for smart cities based on ZigBee wireless sensor network," in *Proc. IEEE IWCMC*, Aug. 2015, pp. 702–707.

[11] J. Chen, Q. Yu, B. Chai, Y. Sun, Y. Fan, and X. Shen, "Dynamic channel assignment for wireless sensor networks: A regret matching based approach," *IEEE Trans. Parallel Distrib. Syst.*, vol. 26, no. 1, pp. 95–106, Jan. 2015.

[12] J. Zheng, Y. Cai, X. Shen, Z. Zheng, and W. Yang, "Green energy optimization in energy harvesting wireless sensor networks," *IEEE Commun. Mag.*, vol. 53, no. 11, pp. 150–157, Nov. 2015.

[13] D. Zhang *et al.*, "Energy harvesting-aided spectrum sensing and data transmission in heterogeneous cognitive radio sensor network," *IEEE Trans. Veh. Technol.*, to be published, doi: 10.1109/TVT.2016.2551721.

[14] N. Zhang, H. Liang, N. Cheng, Y. Tang, J. W. Mark, and X. Shen, "Dynamic spectrum access in multi-channel cognitive radio networks," *IEEE J. Sel. Areas Commun.*, vol. 32, no. 11, pp. 2053–2064, Nov. 2014.

[15] J. Chen, W. Xu, S. He, Y. Sun, P. Thulasiraman, and X. Shen, "Utility-based asynchronous flow control algorithm for wireless sensor networks," *IEEE J. Sel. Areas Commun.*, vol. 28, no. 7, pp. 1116–1126, Sep. 2010.

[16] W. Xu, Y. Zhang, Q. Shi, and X. Wang, "Energy management and cross layer optimization for wireless sensor network powered by heterogeneous energy sources," *IEEE Trans. Wireless Commun.*, vol. 14, no. 5, pp. 2814–2826, May 2015.

[17] L. Huang and M. J. Neely, "Utility optimal scheduling in energy-harvesting networks," *IEEE/ACM Trans. Netw.*, vol. 21, no. 4, pp. 1117–1130, Aug. 2013.

[18] R.-S. Liu, P. Sinha, and C. E. Koksal, "Joint energy management and resource allocation in rechargeable sensor networks," in *Proc. IEEE INFOCOM*, Mar. 2010, pp. 1–9.

[19] Y. Zhang, S. He, J. Chen, Y. Sun, and X. Shen, "Distributed sampling rate control for rechargeable sensor nodes with limited battery capacity," *IEEE Trans. Wireless Commun.*, vol. 12, no. 6, pp. 3096–3106, Jun. 2013.

[20] Y. Zhang, S. He, and J. Chen, "Data gathering optimization by dynamic sensing and routing in rechargeable sensor networks," *IEEE/ACM Trans. Netw.*, vol. 24, no. 3, pp. 1632–1646, Jun. 2016.

[21] R. Urgaonkar and M. J. Neely, "Opportunistic scheduling with reliability guarantees in cognitive radio networks," *IEEE Trans. Mobile Comput.*, vol. 8, no. 6, pp. 766–777, Jun. 2009.

[22] M. Ozger, E. Fadel, and O. B. Akan, "Event-to-sink spectrum-aware clustering in mobile cognitive radio sensor networks," *IEEE Trans. Mobile Comput.*, vol. 15, no. 9, pp. 2221–2233, Sep. 2016.

[23] H. Li *et al.*, "Utility-based cooperative spectrum sensing scheduling in cognitive radio networks," *IEEE Trans. Veh. Technol.*, to be published, doi: 10.1109/TVT.2016.2532886.

[24] Y. Qin *et al.*, "Opportunistic scheduling and channel allocation in MC-MR cognitive radio networks," *IEEE Trans. Veh. Technol.*, vol. 63, no. 7, pp. 3351–3368, Sep. 2014.

[25] H. Sun, A. Nallanathan, C.-X. Wang, and Y. Chen, "Wideband spectrum sensing for cognitive radio networks: A survey," *IEEE Wireless Commun.*, vol. 20, no. 2, pp. 74–81, Apr. 2013.

[26] R. Deng, Y. Zhang, S. He, J. Chen, and X. Shen, "Maximizing network utility of rechargeable sensor networks with spatiotemporally coupled constraints," *IEEE J. Sel. Areas Commun.*, vol. 34, no. 5, pp. 1307–1319, May 2016.

[27] R. Deng, J. Chen, C. Yuen, P. Cheng, and Y. Sun, "Energy-efficient cooperative spectrum sensing by optimal scheduling in sensor-aided cognitive radio networks," *IEEE Trans. Veh. Technol.*, vol. 61, no. 2, pp. 716–725, Feb. 2012.

[28] M. J. Neely, *Stochastic Network Optimization With Application to Communication and Queueing Systems*. San Rafael, CA, USA: Morgan & Claypool, 2010.

[29] L. Huang and M. J. Neely, "Utility optimal scheduling in processing networks," *Perform. Eval.*, vol. 68, no. 11, pp. 1002–1021, 2011.

[30] G. A. Shah, F. Alagoz, E. A. Fadel, and O. B. Akan, "A spectrum-aware clustering for efficient multimedia routing in cognitive radio sensor networks," *IEEE Trans. Veh. Technol.*, vol. 63, no. 7, pp. 3369–3380, Sep. 2014.

[31] S. Boyd and L. Vandenberghe, *Convex Optimization*. Cambridge, U.K.: Cambridge Univ. Press, 2004.

[32] L. Ramshaw and R. E. Tarjan, "On minimum-cost assignments in unbalanced bipartite graphs," HP Labs, Palo Alto, CA, USA, Tech. Rep. HPL-2012-40R1, 2012.

[33] Y. Cui, V. K. N. Lau, R. Wang, H. Huang, and S. Zhang, "A survey on delay-aware resource control for wireless systems—Large deviation theory, stochastic Lyapunov drift, and distributed stochastic learning," *IEEE Trans. Inf. Theory*, vol. 58, no. 3, pp. 1677–1701, Mar. 2012.

Deyu Zhang (S'16) received the B.Sc. degree in communication engineering from PLA Information Engineering University in 2005 and the M.Sc. degree in communication engineering from Central South University, China, in 2012, where he is currently pursuing the Ph.D. degree in computer science. He has been a Visiting Scholar with the Department of Electrical and Computer Engineering, University of Waterloo, Waterloo, ON, Canada, from 2014 to 2016. His research interests include stochastic resource allocation in wireless sensors network and cloud radio access

Zhigang Chen (M'12) received the B.Sc., M.Sc., and Ph.D. degrees in computer science from Central South University (CSU), China, in 1984, 1987, and 1998, respectively. He is a Professor and a Ph.D. Supervisor with CSU. His research interests are in network computing and distributed processing.

Mohamad Khattar Awad (S'02–M'09) received the B.A.Sc. degree in electrical and computer engineering (communications option) from the University of Windsor, Windsor, ON, Canada, in 2004, and the M.A.Sc. and Ph.D. degrees in electrical and computer engineering from the University of Waterloo, Waterloo, ON, Canada, in 2006 and 2009, respectively. From 2004 to 2009, he was a Research Assistant with the Broadband Communications Research Group, University of Waterloo. From 2009 to 2012, he was an Assistant Professor of Electrical and Computer Engineering with the American University of Kuwait. Since 2012, he has been with Kuwait University as an Assistant Professor of Computer Engineering.

Dr. Awad research interests include wireless and wired communications, software-defined networks resource allocation, wireless networks resource allocation, and acoustic vector-sensor signal processing. He received the Ontario Research and Development Challenge Fund Bell Scholarship in 2008 and 2009, respectively, the University of Waterloo Graduate Scholarship in 2009, and a Fellowship Award from the Dartmouth College, Hanover, NH, USA, in 2011. In 2015, he received the Kuwait University Teaching Excellence Award.

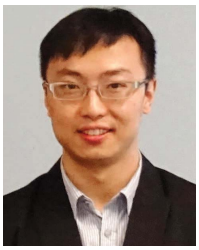

Ning Zhang (M'16) received the B.Sc. degree from Beijing Jiaotong University in 2007, the M.Sc. degree from the Beijing University of Posts and Telecommunications, Beijing, China, in 2010, and the Ph.D. degree from the University of Waterloo, Waterloo, ON, Canada, in 2015. He is currently a Post-Doctoral Research Fellow with the Broadband Communications Research Group, University of Waterloo. His current research interests include next generation wireless networks, software defined networking, green communication, and physical layer security.

Haibo Zhou (M'14) received the Ph.D. degree in information and communication engineering from Shanghai Jiaotong University, Shanghai, China, in 2014. He is currently a Post-Doctoral Fellow with the Broadband Communications Research Group, University of Waterloo. His current research interests include resource management and protocol design in cognitive radio networks and vehicular networks.

Xuemin (Sherman) Shen (M'97-SM'02-F'09) received the B.Sc. (1982) degree from Dalian Maritime University (China) and the M.Sc. (1987) and Ph.D. degrees (1990) from Rutgers University, NJ, USA, all in electrical engineering. He is a Professor and University Research Chair, Department of Electrical and Computer Engineering, University of Waterloo, Canada. He is also the Associate Chair for Graduate Studies. Dr. Shen's research focuses on resource management in interconnected wireless/wired networks, wireless network security, social networks, smart grid, and vehicular ad hoc and sensor networks. He is an elected member of the IEEE ComSoc Board of Governors, and the Chair of HYPERLINK "http://www.comsoc.org/about/memberprograms/distinguished-lecturers" Distinguished Lecturers Selection Committee. Dr. Shen served as the Technical Program Committee Chair/Co-Chair for IEEE Globecom'16, Infocom'14, IEEE VTC'10 Fall, and Globecom'07, the Symposia Chair for IEEE ICC'10, the Tutorial Chair for IEEE VTC'11 Spring and IEEE ICC'08, the General Co-Chair for ACM Mobihoc'15, Chinacom'07 and QShine'06, the Chair for IEEE Communications Society Technical Committee on Wireless Communications, and P2P Communications and Networking. He also serves/served as the Editor-in-Chief for *IEEE Network, Peer-to-Peer Networking and Application*, and *IET Communications*; an Associate Editor-in-Chief for IEEE INTERNET OF THINGS JOURNAL, a Founding Area Editor for IEEE TRANSACTIONS ON WIRELESS COMMUNICATIONS; an Associate Editor for IEEE TRANSACTIONS ON VEHICULAR TECHNOLOGY, *Computer Networks*, and *ACM/Wireless Networks*, etc.; and the Guest Editor for IEEE JSAC, *IEEE Wireless Communications, IEEE Communications Magazine*, and *ACM Mobile Networks and Applications,* etc. Dr. Shen received the Excellent Graduate Supervision Award in 2006, and the Outstanding Performance Award in 2004, 2007, 2010, and 2014 from the University of Waterloo, the Premier's Research Excellence Award (PREA) in 2003 from the Province of Ontario, Canada, and the Distinguished Performance Award in 2002 and 2007 from the Faculty of Engineering, University of Waterloo. Dr. Shen is a registered Professional Engineer of Ontario, Canada, an IEEE Fellow, an Engineering Institute of Canada Fellow, a Canadian Academy of Engineering Fellow, a Royal Society of Canada Fellow, and a Distinguished Lecturer of IEEE Vehicular Technology Society and Communications Society.